Proceedings of ICTACEM 2007
International Conference on Theoretical, Applied, Computational and Experimental Mechanics
December 27-29, 2007, IIT Kharagpur, India
ICTACEM-2007/0227

Relative assessment of different turbulence models in prediction of airfoil characteristics for a wide range of angle of attack

D.S.Kulkarni[a], S.Sarkar[b] and Sekhar Majumdar[c*]

[a] Scientist, CTFD Division, National Aerospace Laboratories, Bangalore, India
[b] Associate Prof, Deptt of Mech Engg, Indian Institute of Technology, Kanpur, India
[c] Scientist, CTFD Division, National Aerospace Laboratories, Bangalore, India

ABSTRACT

Simulation of separated flow past an airfoil beyond stall, along with the prediction of stall itself still remains a challenging problem. In practical design and analysis problems of aerodynamics involving turbulent flow, the most widely used methodology is the numerical solution of the Reynolds Averaged Navier Stokes (RANS) in conjunction with appropriate closure models to represent the effect of turbulent stresses. The present paper attempts to compute flow past a symmetric airfoil for a wide range of angles of attack using the code RANS3D developed at NAL Bangalore. The RANS code is coupled to three different eddy viscosity based turbulence models - *viz.*, the low *Re* version of the k-ε model, low *Re* version of $k-\omega$ model and the $\overline{v^2}-f$ model, for which the ability to capture the massive flow separation at and beyond stall has been carefully examined for an operating chord-based Reynolds number of 2 to 3 million and the angle of attack varying from 0 to 25 degrees. Validation against measurement data for instantaneous flow field indicate that all the turbulence models perform almost equally well in pre-stall regimes, while some uncertainties are observed when the flow becomes highly unsteady for high angle of attack. The vortex shedding from the upper surface of the airfoil leading to massive separated flow structure is captured by all the turbulence models. As far as the mean lift and drag coefficients are concerned, reasonable agreement is observed between the low *Re* k-ε & low Re $k-\omega$ model prediction and the measurement data whereas the $\overline{v^2}-f$ model, in general, has a tendency of overpredicting the aerodynamic coefficients. The Strouhal number, indicating the frequency of the periodic vortex shedding behavior, is observed to be not so sensitive to the turbulence model used for computation.

Keywords: Multiblock Boundary Conforming Grid, Pressure-Velocity solution strategy, Implicit RANS solver, Unsteady Flow, Eddy Viscosity based Turbulence Models

1. INTRODUCTION

The assessment of turbulence models in predicting flow fields that are directly relevant to industrial needs has become increasingly important. In aerodynamics, the simulation of separated flow past an airfoil beyond stall, along with the prediction of stall itself, is a very challenging problem. Panel methods and inviscid Euler computations, which have been routinely used for aerodynamic design in industry, are unable to predict flow separation and

* Further author information:
D.S.K: E-mail: dsk@ctfd.cmmacs.ernet.in, Telephone: +91-80-25051608
S.S : E-mail: subra@iitk.ac.in, Telephone: +91-512-2597942
S.M : E-mail: sekhar@ctfd.cmmacs.ernet.in, Telephone: +91-80-25051617

stall. An extensive reliance on wind tunnel measurements is still required for the design of airfoils where flows are highly unsteady with complex turbulent structures. Although, DNS is often employed to predict the turbulent flows, the computation cost is prohibitive. Even LES is also expensive for practical flow environments at moderate Reynolds numbers. Since designers are primarily interested in the time averaged values of shear stress, pressure and velocity rather than the time dependent details, practical design and analysis can often be obtained using the Reynolds Averaged Navier Stokes (RANS) equations in conjunction with appropriate closure models to represent the effect of turbulent stresses. The present paper attempts to compute flow past a symmetric airfoil for various angles of attack, using a RANS solver[1], coupled to three different eddy viscosity based turbulence models. The ability of these models to capture the massive flow separation beyond stall along with the stall itself has been carefully examined

2. FINITE VOLUME METHOD

2.1 Governing equations

The instantaneous Navier Stokes equations for unsteady incompressible flow may be written in a coordinate-free form as follows:

Mass Conservation (Continuity):

$$div(\rho U) = 0 \tag{1}$$

Momentum Conservation:

$$\frac{\partial(\rho U)}{\partial t} + div(\rho U \otimes U) = -grad\ p + \mu \nabla^2 U + S \tag{2}$$

where, p, μ and ρ are the pressure, viscosity and density respectively, U is the instantaneous velocity vector and S is any source term other than pressure gradient. The gradient (*grad*) and divergence (*div*) terms may be further expanded in terms of the geometrical coefficients depending on the coordinate system used. Now using the Reynolds decomposition for unsteady turbulent flow:

$$U = \langle U \rangle + u \tag{3}$$

where $\langle U \rangle$ is the ensemble-averaged velocity vector and u is the fluctuating velocity vector. Substitution of U from Eq. 3, followed by ensemble averaging transforms the mass conservation and the momentum equations as:

$$div(\rho\langle U\rangle) = 0 \tag{4}$$

$$\frac{\partial(\ \rho\langle U\rangle\ )}{\partial t} + div(\ \rho\langle U\rangle \otimes \langle U\rangle\ ) = -grad\ \langle p\rangle + \mu\nabla^2\langle U\rangle - div(\ \rho\langle u\rangle \otimes \langle u\rangle\ ) + \langle S\rangle \tag{5}$$

The unknown correlation term $-\rho\langle u\rangle \otimes \langle u\rangle$ is known as the Reynolds stress tensor for which each component $-\rho\langle u_i u_j\rangle$ is evaluated through some appropriate turbulence models discussed later. In a structured curvilinear 3D grid environment, a typical hexahedral shaped control volume is formed by piecewise linear segments joining the eight cell corners, determined by a suitable grid generation procedure and all the flow variables are stored at the geometric center of each control volume.

2.2 Turbulence Model

The turbulence models used and validated extensively for engineering flows are based on the Eddy Viscosity Hypothesis which expresses the second moment correlation of fluctuation due to turbulence as product of an eddy viscosity and the mean strain rate as follows:

$$-\rho\langle u_i u_j\rangle = \mu_t\left[\frac{\partial\langle U_i\rangle}{\partial x_j} + \frac{\partial\langle U_j\rangle}{\partial x_i}\right] - \frac{2}{3}\rho\delta_{ij}k \tag{6}$$

where, δ_{ij} is the Kronecker delta and k is the turbulence kinetic energy. The eddy viscosity μ_t is assumed to be an isotropic scalar quantity whose value depends on the local state of turbulence. Eddy viscosity may be expressed as the product of fluid density, a characteristic length scale and a characteristic velocity scale. In the $k-\varepsilon$ model, for example, μ_t, the turbulent or eddy viscosity is defined as :

$$\mu_t = \rho\, f_\mu C_\mu\, k^2/\varepsilon \tag{7}$$

The present paper explores three different advanced turbulence models which compute the eddy viscosity by solving separate transport equations for the turbulent velocity and length scales.

2.2.1 Low Re $k-\varepsilon$ Model

This two equation model, proposed by Chien[2], has been designed to maintain the high *Re k-ε* formulation in the log law region and at the same time tuned through exponential damping functions to fit in the viscous and buffer layers. A damping function f_μ is introduced in the definition of the eddy viscosity to mimic the direct effect of molecular viscosity on the shear stress. The near wall turbulence energy and its dissipation are also modified through exponential functions of the wall-normal distance. The relevant transport equations of the model in simple cartesian coordinates and the special functions used are as follows:

Transport equation for turbulent kinetic energy (k) :

$$\frac{\partial(\rho k)}{\partial t} + div(\rho \langle U \rangle k) = P_k - \rho\tilde{\varepsilon} + \nabla\left[\left(\mu_l + \frac{\mu_t}{\sigma_k}\right)\nabla k\right] - D \tag{8}$$

where the production of turbulence kinetic energy P_k is expressed as:

$$P_k = \mu_t\left[\frac{\partial\langle U_i\rangle}{\partial x_j} + \frac{\partial\langle U_j\rangle}{\partial x_i}\right]\frac{\partial\langle U_i\rangle}{\partial x_j} \tag{9}$$

Transport equation for turbulence dissipation ($\tilde{\varepsilon}$) :

$$\frac{\partial(\rho\tilde{\varepsilon})}{\partial t} + div(\rho\langle U\rangle\tilde{\varepsilon}) = f_1 C_{\varepsilon 1} P_k \frac{\tilde{\varepsilon}}{k} - f_2 C_{\varepsilon 2}\rho\frac{\tilde{\varepsilon}^2}{k} + \nabla\left[\left(\mu_l + \frac{\mu_t}{\sigma_\varepsilon}\right)\nabla\tilde{\varepsilon}\right] - E \tag{10}$$

$$\mu_t = \rho f_\mu C_\mu k^2 / \tilde{\varepsilon} \tag{11}$$

where, *D* and *E* are special terms and f_μ f_1 and f_2 are exponential damping functions to account for the low Reynolds number effects in the vicinity of the wall and these functions are discussed in details by Chien[2].

Stagnation point anomaly

The standard $k-\varepsilon$ model based on isotropic eddy viscosity concept usually produces an excessive level of k and μ_t near a stagnation point, often encountered in the vicinity of a stagnation zone. Kato & Launder[3] suggested an ad-hoc measure to replace the original production term $P_k = 2\mu_t |S|^2$ in the k-transport equation (Eq. 8) by $P_k = 2\mu_t |S||\Omega|$ where $|S|$ & $|\Omega|$ are the magnitude of the mean strain rate S and the vorticity Ω respectively. The vorticity near stagnation zones is usually low due to almost irrotational bending of the fluid and hence the calculated values of unrealistic high level of turbulence energy may be avoided.

2.2.2 Low Re $k-\omega$ Model

In $k-\omega$ turbulence model, a transport equation for specific dissipation (ω) is solved instead of solving a transport equation for ε as in the case of $k-\varepsilon$ model and the transport equations for k and ω are integrated all the way up to the wall. In order to produce accurate near wall predictions of kinetic energy and eddy viscosity, exponential damping functions f_1, f_2 and f_μ are used in the equations of k, ω and μ_t to account for the low Reynolds number effects in the vicinity of the wall and are discussed in details by Jones[4]. The modelled transport equations for the low Reynolds number $k-\omega$ turbulence model are written as follows:

Transport equation for turbulent kinetic energy (k) is :

$$\frac{\partial(\rho k)}{\partial t} + div(\rho \langle U \rangle k) = P_k - f_1 \rho \omega k + \nabla\left[\left(\mu_l + \frac{\mu_t}{\sigma_k}\right)\nabla k\right] \tag{12}$$

Transport equation for specific dissipation (ω) is :

$$\frac{\partial(\rho \omega)}{\partial t} + div(\rho \langle U \rangle \omega) = C_{\omega 1} P_k \frac{\omega}{k} - f_2 C_{\omega 2} \rho \omega^2 + \nabla\left[\left(\mu_l + \frac{\mu_t}{\sigma_\omega}\right)\nabla \omega\right] \tag{13}$$

$$\mu_t = \rho f_\mu C_\mu k / \omega \tag{14}$$

2.2.3 $\overline{v^2} - f$ *Model*

The $\overline{v^2} - f$ turbulence model, originally proposed by Durbin[5] has become increasingly popular due to its ability to correctly account for near wall damping without use of ad-hoc damping functions. In the $\overline{v^2} - f$ model two additional equations, one for the wall-normal component of the Reynolds stress ($\overline{v^2}$) and another for a redistribution function (f) are solved in addition to the k and ε-equations (Eqs. 8 and 10) without any ad-hoc damping function. The equation for f is a Helmholtz kind of elliptic equation, derived from the Poisson equation satisfying the fluctuating pressure field.

Transport equation for ($\overline{v^2}$) is :

$$\frac{\partial(\rho\overline{v^2})}{\partial t} + div(\rho\langle U\rangle\overline{v^2}) = \rho k f - 6\rho\frac{\overline{v^2}}{k}\varepsilon + \nabla\left[(\mu_l + \mu_t)\nabla\overline{v^2}\right] \tag{15}$$

Transport equation for Redistribution function (f) is :

$$L^2\nabla^2 f - f = \frac{1}{T}\left[(C_1 - 6)\frac{\overline{v^2}}{k} - \frac{2}{3}(C_1 - 1)\right] - C_2\frac{P_k}{k} \tag{16}$$

Durbin[5] observed that the turbulent viscosity is largely over predicted by the $k-\varepsilon$ model in the near wall region because the variation of $k \propto y^2$ is rather slow to account for the rapid variation of the μ_t in the near wall region. On the other hand $\overline{v^2}$ provides a better velocity scale as its variation ($\overline{v^2} \propto y^4$) is rapid in the near wall region due to the kinematic blocking by the impermeable wall. So the eddy viscosity is redefined in which $\overline{v^2}$ is used as a velocity scale instead of the turbulent kinetic energy (k), to evaluate the turbulent viscosity μ_t as:

$$\mu_t = \rho C_\mu \overline{v^2} T \tag{17}$$

where, the time scale T and the length scale L are expressed in the following limiter form :

$$T = \max\left[\frac{k}{\varepsilon}, 6\left(\frac{\nu}{\varepsilon}\right)^{\frac{1}{2}}\right] \tag{18}$$

$$L = C_L \max\left[\frac{k^{\frac{3}{2}}}{\varepsilon}, C_\eta\left(\frac{\nu^3}{\varepsilon}\right)^{\frac{1}{4}}\right] \tag{19}$$

2.3 Numerical Simulaion Method

The present computation uses a general geometry, block structured, pressure-based implicit finite volume algorithm RANS3D[1,6], developed at the CTFD Division, NAL Bangalore . A third order accurate QUICK[7] scheme along with few low diffusive high order upwind schemes coupled to a deferred correction procedure[8] has been used for both convective and diffusive fluxes. The detailed algebra of the schemes is discussed elsewhere[9]. An iterative decoupled approach similar to the SIMPLE algorithm[10], modified for collocated variable arrangement[11] is adopted to avoid the checkerboard oscillations of the flow variables. The system of linear equations derived from the finite volume procedure is solved sequentially for the velocity components, pressure correction and turbulence scalars using the strongly implicit procedure of Stone[12].

4. RESULTS AND DISCUSSION

A two-block C-type grid (Fig.1) is used around the NACA0012 airfoil and the far field is placed at a distance of 10C where C is the chord length. The y^+ of the first near wall grid point is maintained to be less than 0.5. Initial parametric study has been carried out for the grid independency and for the effect of convective flux discretisation schemes on the accuracy. Based on this sensitivity study, The QUICK scheme is used for flux discretisation for all the computations with a 527x121 grid where the grid nodes are divided into two blocks- one covering the wake zone with 125 nodes along the wake and 241 nodes along the transverse direction and the other block covering the airfoil surface by 279 nodes and 121 nodes along the transverse direction. Fig. 2 shows a very good agreement between the measurement data[13] and the present computation results for the surface pressure distribution at a flow Reynolds number of 3 million and at two different angles of attack (α =8^0 and 15^0). The variation of lift coefficient with angle of attack shown in Fig. 3 demonstrates that the magnitude of the maximum lift is predicted more accurately by the low *Re* $k-\varepsilon$ and $\overline{v^2}-f$ model; however both the models predict the location of the maximum lift at about 18^0,

compared to 16^0 observed in measurement. Fig. 4 shows the particle traces based on the computed time-averaged velocity field employing $\overline{v^2}-f$ turbulence model at two different angles of attack (α =12^0 and 20^0). In both the cases the time-accurate computation of the flow is observed to be reaching a steady state. However in case of α =12^0, the flow remains attached over the whole length of the airfoil up to the trailing edge whereas in case of α =20^0 the flow separates just before the trailing edge and reattaches once again forming a small separation bubble.

In the next step the value of angle of attack (α) is increased to 25^0 for which measurement data[14] is available for the aerodynamic coefficients at a Reynolds number of 2 million. In this case the time accurate computation shows the flow to be unsteady and periodic in nature with a dominant frequency. The phenomenon of vertex shedding from the upper surface of the airfoil is clearly observed in the instantaneous particle traces as shown in Fig. 5 by the $\overline{v^2}-f$ turbulence model at four different instants of the shedding cycle of time period. The flow patterns derived from other two turbulence models also look qualitatively in a similar fashion. However the temporal evolution of lift and drag coefficients for computation using different turbulence models, shown in Fig. 6 and Fig. 7 respectively, illustrate that $\overline{v^2}-f$ model predicts a higher amplitude of fluctuation of the aerodynamic coefficients, compared to the low *Re* $k-\varepsilon$ and $k-\omega$ model prediction. The summary of spectral analysis (FFT) of the time signal for the aerodynamic coefficients is shown in Table 1. and the mean value of the coefficients predicted by low *Re* $k-\varepsilon$ and low *Re* $k-\omega$ model are observed to match well with the measurement data[14], whereas the $\overline{v^2}-f$ model overpredicts the mean coefficients by about 20%. The Strouhal number ($St = C/U_\infty T$), which indicates the frequency of the periodic vortex shedding, however is observed to be not so sensitive to the turbulence model used for the computation.

Instantaneous vorticty contours are shown in Figs 8, 9 and 10 for the low *Re* version of $k-\varepsilon$, low *Re* $k-\omega$ and the $\overline{v^2}-f$ turbulence models respectively and a regular vortex shedding pattern is clearly visible. It may be noted that the contour scale is limited to values of ± 10 and the values of vorticity near the wall are as high as -14000 to +10000; however the interest lies here in the vortex shedding. The vorticity contours are found to be quite consistent with the corresponding streamline patterns of the respective turbulence model.

Figs. 11, 12 and 13 show typical instantaneous contours of turbulent kinetic energy (k) using the low $Re\ \ k-\varepsilon$, low $Re\ \ k-\omega$ and $\overline{v^2}-f$ turbulence models respectively. The high turbulent kinetic energy area is observed to occur near the trailing edge on the suction side and also in the near wake between X/C=1.0 to X/C=2.0. The zone of high turbulent kinetic energy more or less matches with the regions of the vortex core observed on the suction surface and the wake. The levels of instantaneous turbulent kinetic energy predicted by $\overline{v^2}-f$ model appear to be somewhat lower than those predicted by the low $Re\ \ k-\varepsilon$ and low $Re\ \ k-\omega$ models. The computed results indicate that all the three turbulence models perform equally well in the pre-stall flow regime, while there are uncertainties when the flow becomes highly unsteady for high angle of attack. However the overall results illustrate that the RANS simulations can be used for prediction of the time-averaged aerodynamic characteristics, even at moderately high angle of attack beyond the stall condition.

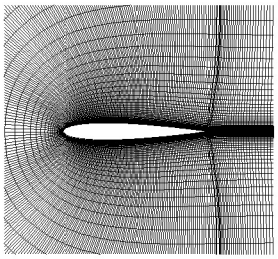

Figure 1. 2-Block C-grid around NACA0012 airfoil (527x121, Near wall $y^+<0.5$)

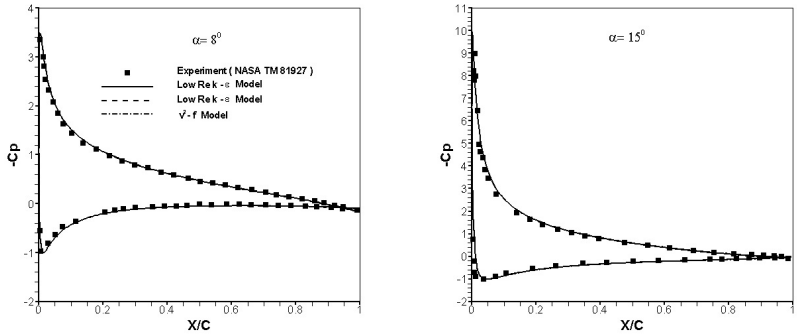

Figure 2. Chord wise variation of surface pressure distribution for different turbulence models (Re=3x10^6)

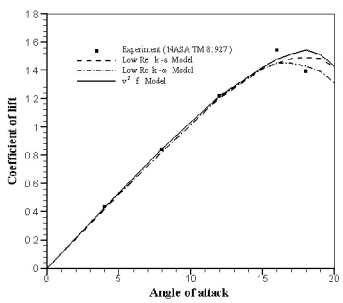

Figure 3. Variation of C_l with angle of attack for different turbulence models (Re=3x10^6)

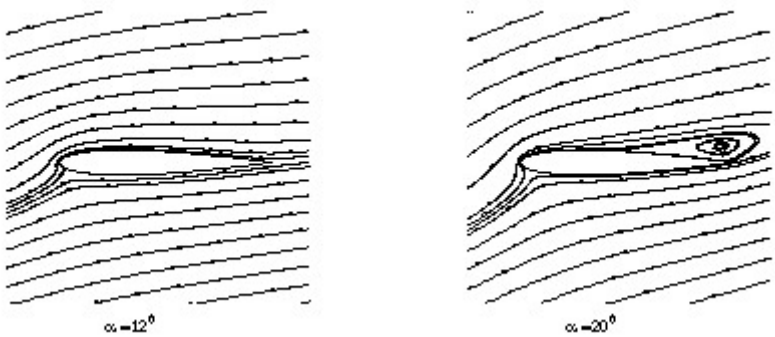

Figure 4. Computed streamlines pattern ($\overline{v^2}-f$ Model, Re=3x10^6)

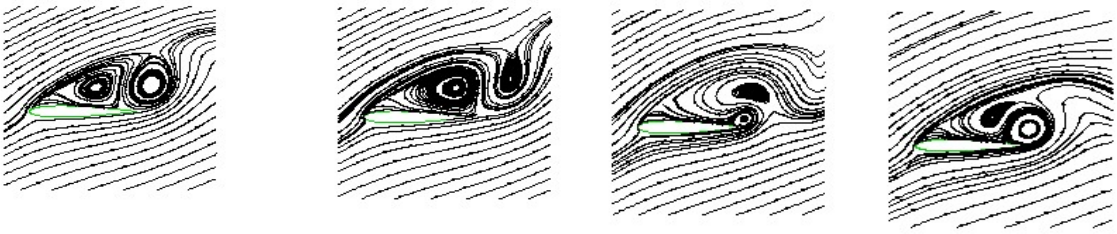

(a) t =T/4 (b) t=T/2 (c) t=3T/4 (d) t=T

Figure 5. Instantaneous flow pattern for flow around NACA0012 airfoil ($\overline{v^2} - f$ Model, α =25^0 ,Re=$2x10^6$)

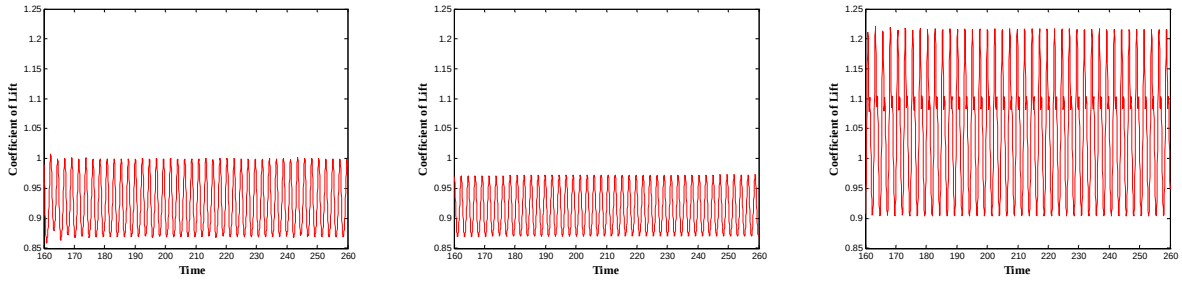

(a) Low *Re* k-ε Model (b) Low *Re* k-ω Model (c) $\overline{v^2}$ - f Model

Figure 6. Temporal variation of coefficient of lift for different turbulence models (α =25^0 , *Re* = $2x10^6$)

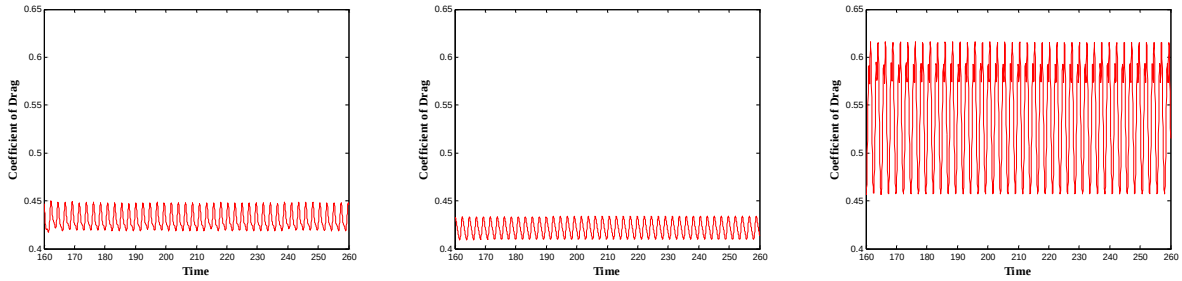

(a) Low *Re* k-ε Model (b) Low *Re* k-ω Model (c) $\overline{v^2}$ - f Model

Figure 7. Temporal variation of coefficient of drag for different turbulence models (α =25^0 ,*Re* = $2x10^6$)

Table 1. Mean values of C_l and C_d for different turbulence models (Re = $2x10^6$, α =25^0)

	Mean C_l	Mean Cd	Strouhal No.
Low *Re* k-ε Model	0.9262	0.4308	0.4297
Low *Re* k- ω Model	0.9165	0.4213	0.4297
$\overline{v^2} - f$ Model	1.0466	0.5398	0.4102
Experiment (SAND80-2114)	0.9352	0.4200	----------

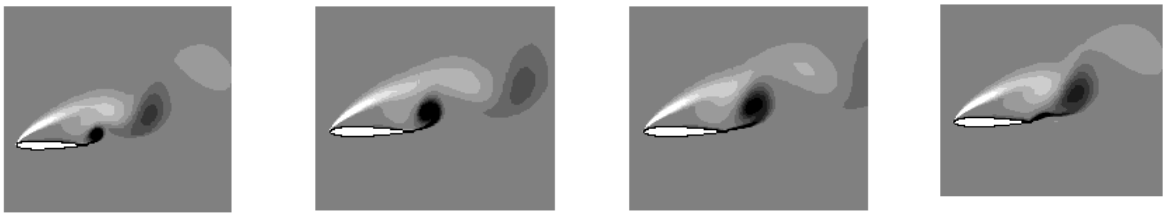

(a) t =T/4 (b) t=T/2 (c) t=3T/4 (d) t=T

Figure 8. Instantaneous vorticity contours for Low Re $k-\varepsilon$ model in a vortex shedding cycle (α =25^0 , Re=2x10^6, T=Time period)

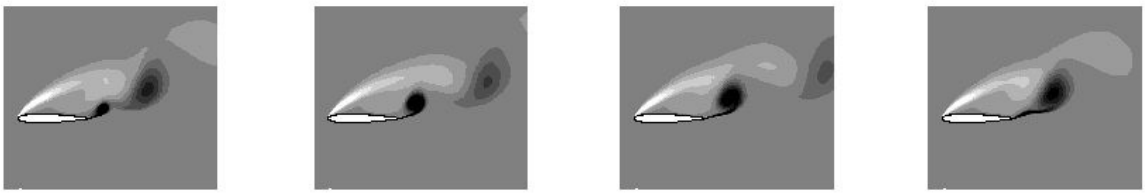

(a) t =T/4 (b) t=T/2 (c) t=3T/4 (d) t=T

Figure 9. Instantaneous vorticity contours for Low Re $k-\omega$ model in a vortex shedding cycle (α =25^0 , Re=2x10^6, T=Time period)

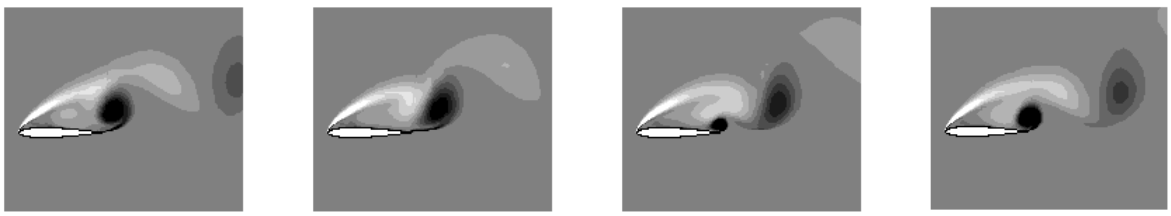

(a) t =T/4 (b) t=T/2 (c) t=3T/4 (d) t=T

Figure 10. Instantaneous vorticity contours for $\overline{v^2}-f$ model in a vortex shedding cycle (α =25^0 , Re=2x10^6, T=Time period)

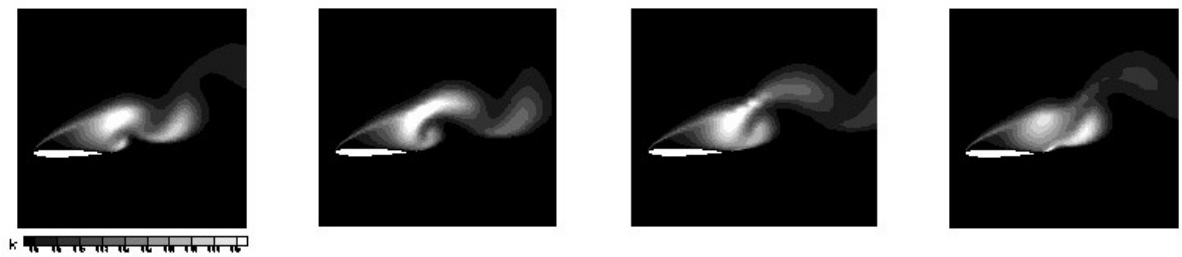

(a) t =T/4 (b) t=T/2 (c) t=3T/4 (d) t=T

Figure 11. Instantaneous turbulent kinetic energy contours for Low Re $k-\varepsilon$ model in a vortex shedding cycle (α =25^0 , Re=2x10^6, T=Time period)

(a) t =T/4 (b) t=T/2 (c) t=3T/4 (d) t=T

Figure 12. Instantaneous turbulent kinetic energy contours for Low Re $k-\omega$ model in a vortex shedding cycle (α =25^0 , Re=2x10^6, T=Time period)

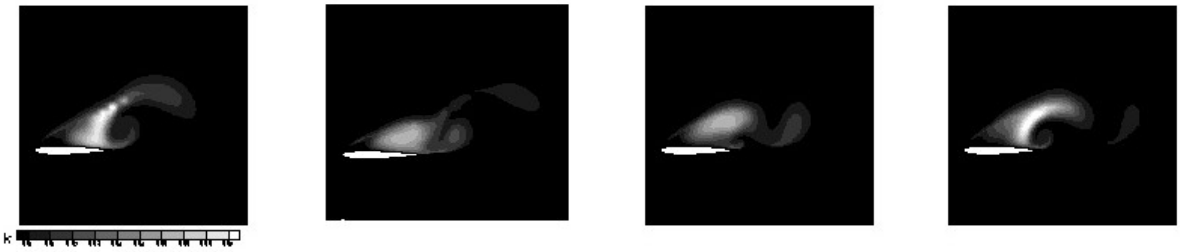

(a) t =T/4 (b) t=T/2 (c) t=3T/4 (d) t=T

Figure 13. Instantaneous turbulent kinetic energy contours for $\overline{v^2}-f$ model in a vortex shedding cycle (α =25^0 , Re=2x10^6, T=Time period)

5. CONCLUSION

Simulations of turbulent flow over a NACA0012 airfoil have been carried out successfully using the RANS3D code, coupled to different turbulence models for a wide range of angles of attack operating at a chord-based Reynolds numbers of 2 to 3 million. The magnitude of the maximum lift coefficient at the stall condition is predicted reasonably well by low *Re* $k-\varepsilon$ and $\overline{v^2}-f$ turbulence models but the stall angle is overpredicted by about 2^0 compared to the corresponding measurement data. The phenomenon of vortex shedding leading to massive flow separation in the post-stall regime, observed in measurement, has been captured reasonably well. As far as the mean aerodynamic coefficients are concerned, the low *Re* $k-\varepsilon$ and $k-\omega$ model results are found to be in closer agreement to measurement data than the $\overline{v^2}-f$ model results.

ACKNOWLEDGMENTS

The authors wish to thank the Director NAL, Bangalore and Director IIT, Kanpur for permission to publish this paper.

REFERENCES

1. S. Majumdar, B.N.Rajani, D.S.Kulkarni, S.Mohan, "RANS computation of low speed turbulent flow in complex configuration," *Proc. Symposium on state-of-the-art and future Trends of CFD at NAL*. NAL SP 0301,2003
2. K.Y. Chien, "Predictions of channel and boundary layers flows with a low Reynolds no. turbulence model," *AIAA Journal*. 20:33-38,1982
3. M.Kato, B.E. Launder, "The Modeling of turbulent flow around stationary and vibrating square cylinder," *Proc. 9th Symposium Turbulent Shear Flows* , Kyoto, 1993
4. R.M. Jones, "Advanced turbulence modeling for industrial flows," *Ph.D Thesis* Louisiana state University, 2003
5. P.A. Durbin, "Separated flows computation with the $k-\varepsilon-\overline{v^2}-f$ model," *AIAA Journal*. 33:644-659, 1995
6. S. Majumdar, W. Rodi, J.Zhu, "Three dimensional finite volume method for incompressible flows with complex boundaries," *Journal of Fluid Engineering , ASME*, 496-503, 1992
7. B.P. Leonard, "A stable and accurate convective modeling procedure based on quadratic interpolation," *Computer Methods in Applied Mechanics Engineering*. 19:59-98,1979
8. P.K. Khosla, S.G.Rubin, "A diagonally dominant second-order accurate implicit scheme," *Computers and Fluids.* 2:207-209, 1974
9. D.S. Kulkarni, B.N. Rajani, S. Majumdar, "Studies on temporal and spatial discretisation schemes used in a Pressure-based RANS algorithm for incompressible flow," *NAL PDCF 0108*, 2001
10. S.V. Patankar, D.B.Spalding, "A calculation procedure for heat, mass and momentum transfer in three-dimensional parabolic flows," *International Journal of Heat and Mass Transfer*, 15: 1787-1806,1972
11. S.Majumdar, "Role of underrelaxation in momentum interpolation for calculation of flow with non-staggered grids," *Numerical Heat Transfer*. 13:125-132,1988
12. H.L. Stone, "Iterative solution of implicit approximations of multidimensional partial differential equations," *SIAM Journal of Numerical Analysis*. 5:530-538,1968
13. D.H.Charles, "Two-dimensional aerodynamic characteristics of the NACA0012 airfoil in the Langley 8-foot transonic pressure tunnel," *NASA TM 81927*, 1981
14. R.E. Sheldahl, P.C. Klimas, "Aerodynamics Characteristics of Seven Airfoil Sections Through 180 Degrees Angle of Attack for use in aerodynamic analysis of vertical axis wind turbines," *SAND80-2114*, Sandia National Laboratories, Albuquerque, 1981